J Amer Oil Chem Soc (2007) 84:621–629
DOI 10.1007/s11746-007-1093-x

ORIGINAL PAPER

The Effect of Emulsifier Type and Droplet Size on Phase Transitions in Emulsified Even-Numbered *n*-Alkanes

İbrahim Gülseren · John N. Coupland

Received: 30 March 2007 / Revised: 6 May 2007 / Accepted: 23 May 2007 / Published online: 21 June 2007

Abstract Phase transitions in emulsified even-numbered *n*-alkanes (C_{16}, C_{18}, and C_{20}) are studied as a function of droplet size (0.15–3.45 μm) and surfactant type (polyoxyethylene sorbitan monolaurate or caseinate) using microcalorimetry (DSC) and ultrasonic attenuation measurements (2.25 MHz). Two DSC exothermic peaks were observed during the heating of C_{18} and C_{20} emulsions stabilized by Tween 20: a minor peak around 15 and 25 °C, respectively, and a major double peak about 10 °C higher. We tentatively attribute the minor peak to crystal-rotator phase transition, and the split major peak to melting of the surface and core of the droplets. The C_{16} emulsions showed similar behavior for the major melting peak (15 °C), but the minor peak was absent-possibly as the sample was not cooled enough to cause the rotator phase to enter the low temperature crystalline state. For similar sodium caseinate stabilized emulsions of C_{18} and C_{20}, the minor peak was much less pronounced (~25%), which we attribute to the lack of compatibility between the alkane and protein molecules. There were two ultrasonic attenuation peaks for the melting of C_{18} and C_{20} and one for C_{16} corresponding to the DSC peaks. In all cases, the magnitude of the attenuation decreased with increasing particle size. Using an extended scattering theory approach we were able to relate the changes in ultrasonic attenuation to the changes in the effective physical properties of the alkane molecules during melting.

İ. Gülseren · J. N. Coupland (✉)
Department of Food Science,
The Pennsylvania State University,
337 Food Science Building,
University Park, PA 16802, USA
e-mail: Coupland@psu.edu

Keywords Low-intensity ultrasound · *n*-Alkane · Emulsions · Scattering theory · Rotator phase · Surfactants

Introduction

The crystallization and melting behavior of the dispersed phase in oil-in-water emulsions has attracted considerable interest both as it is important to the functionality of certain commercial products (e.g., whipped cream) but also as it provides a means to study the basics of nucleation and melting without the complication of crystal growth [1]. Crystallization of emulsified lipids typically requires much more extensive supercooling than the same lipid in bulk, because each droplet must nucleate independently and the influence of heterogeneous catalysts is minimized. For example, Montenegro et al. [2] showed the crystallization temperature of hexadecane in a miniemulsion (218 nm) was 16 °C lower than that of the bulk sample, whereas the melting point decreased only slightly (i.e., 0.7 °C) [3]. The phase behavior of emulsified lipids is affected by the surfactant present at the oil-water interface. Katsuragi et al. [4] argued that if the hydrophobic portion of a small molecule surfactant is structurally similar to the lipid itself, it may catalyze droplet crystallization. On the other hand, the hydrophobic tails of the surfactant can act as impurities for the lipid adjacent to the surface so reducing its melting temperature and consequently, the fat in fine emulsions sometimes melts in two events at different temperatures (i.e., core and surface) [5].

Normal alkanes are frequently used as model lipids for emulsion crystallization studies, as they are readily available over a range of chain lengths to a good degree of purity. Medium chain, even carbon numbered alkanes in emulsions typically crystallize in a triclinic form, although

this can be modified by the addition of high-melting, hydrophobic emulsifiers [6]. However, in recent work we used temperature scanning microcalorimetry to identify a small thermal event occurring about 12 °C below the major melting/crystallization peak of emulsified octadecane [7]. We tentatively attributed this to the melting/formation of a rotator phase as an intermediate between the high temperature liquid and low temperature crystal. A rotator phase is defined as lamellar crystals, "which exhibit long-range order in the molecular axis orientation and center-of-mass position but lack rotational degrees of freedom of the molecules about their long axis" [8]. There was also an excess ultrasonic attenuation on heating the octadecane emulsions associated with the crystal-rotator and rotator-liquid phase transitions [7]. As the droplets melt, their effective specific heat and thermal expansion coefficient are instantaneously very high as they include contributions from the enthalpy of fusion and changing solids content, respectively. By incorporating these terms into scattering theory, it was possible to model the excess attenuation during melting.

In the present work, we extend this investigation to consider a wider range of emulsion samples prepared with different surfactants (i.e., one protein, one small molecule surfactant), oils (i.e., three different *n*-alkanes), and particle sizes. We combine sensitive microcalorimetric measurements of the enthalpy transitions in the samples with ultrasonic attenuation measurements. Our aims are to identify the factors affecting the small transition attributed to the rotator phase as well as the main melting and crystallization events and to demonstrate excess ultrasonic "melting" attenuation in a wider range of samples.

Materials and Methods

Materials and Sample Preparation

n-Octadecane (C_{18}) and *n*-Eicosane (C_{20}) were obtained from Alfa Aesar (99% purity). Tween 20 (polyoxyethylene sorbitan monolaurate, W929150-1) and sodium caseinate were purchased from Aldrich Chemical Company. *n*-Hexadecane (C_{16}) was obtained from Fisher Scientific Company. The alkane (3 wt%) was mixed with a Tween 20 (1 wt%) or sodium caseinate (0.5% wt) solution in a high speed blender (Kinematica GmbH FT10/35, Brinkmann Instruments, Switzerland) to prepare a coarse emulsion, which was further homogenized using a two-stage valve homogenizer (1–5 passes, 200–600 bar, 10% of which was maintained over the second stage, Niro-Soavi Panda, Model no: 3344, Parma, Italy). In order to keep the oil in a liquid state for homogenization, the equipment was preheated with hot water prior to use. The particle size distribution of the emulsions was characterized by static light scattering (Horiba LA-920, Irvine, CA, USA) after appropriate dilution. The emulsions were stable over the course of the experiment (i.e., no change in particle size, no visible phase separation) and were not destabilized by the cooling–heating cycles.

Ultrasonic Measurements

The ultrasonic attenuation of the emulsions was measured as a function of temperature using a modified pulse-echo technique. An electrical spike signal (Panametrics 500 PR, Waltham, MA, USA) was passed to a broadband ultrasonic transducer (2.25 MHz center frequency, Panametrics, Waltham MA), which converted the energy to ultrasound. The pulse of sound traveled into a Plexiglas delay line, and was partially reflected at the plastic-sample interface. The reflected part of the signal returned through the delay line to the transducer (echo 1) and the transmitted part traveled through the sample (~1 cm), was reflected from the brass plate and returned through the sample and the delay line to the transducer (echo 2). The transducer reconverted the acoustic signal to an electrical signal, which was stored for analysis with a digital oscilloscope (LeCroy 9310c, Chestnut Ridge, NY, USA). The time and energy difference between echo 1 and echo 2 were used to calculate the speed of sound and attenuation of the sample.

Aliquots (~20 ml) of C_{16}, C_{18}, and C_{20} emulsions were poured into the ultrasonic measurement cell at 30, 35, and 45 °C, respectively, and held for 30 min, then cooled to 0 °C at 6 °C h^{-1} and measurements were taken at each integer °C. Additional measurements were taken to increase the resolution of the ultrasonic data around the attenuation peaks. To ensure complete crystallization before the heating cycle, the C_{16} samples were held at –5 °C and the C_{18} and C_{20} emulsions at 0 °C for 30 min before reheating at the same rate to the starting temperature. The aqueous phase of the emulsions did not freeze under these conditions.

Differential Scanning Calorimetry

The crystallization and melting thermograms were measured using differential scanning calorimetry (VP-DSC, Microcal, Northampton, MA). Samples were diluted to 0.25 wt% lipids with water prior to analysis so that the signals were within the range of the instrument. Samples (513.1 μl) were run against a similar reference cell filled with water. C_{16}, C_{18}, and C_{20} samples were heated to 30, 35, 45 °C, respectively, held for 30 min, and cooled to 0.5 °C at 10 °C h^{-1} then held for a further 30 min and reheated at the same rate to 30, 35, and 45 °C for C_{16}, C_{18}, and C_{20} samples. The heat capacity data for the water-water scan

was subtracted from the sample runs to measure the heat flux due to changes in the lipid phase. In preliminary experiments, we showed that Tween 20 and sodium caseinate solutions did not exhibit any measurable transitions over this range.

Results and Discussion

Melting Thermograms

The melting behavior of coarse (d_{32} = 3.45 μm), intermediate (d_{32} = 0.45 μm) and fine (d_{32} = 0.15 μm) emulsions of C_{16}, C_{18} and C_{20} stabilized by Tween 20 were monitored by microcalorimetry (Fig. 1). There was a single, large endothermic peak corresponding to the melting of C_{16} whose maximum increased with droplet size (i.e., 16.9, 17.3, and 17.7 °C for fine, intermediate, and coarse emulsions, respectively, Fig. 1a). Various authors [2, 3] have noted a small increase in melting temperature with droplet size and this is usually attributed to a reduction in surface curvature and crystal structure. The peak for the larger droplets was larger, and occurred over a narrower temperature range while the finer droplets had broader melting peaks preceded by a smaller maximum at approximately 15 °C. Our observations are similar to those reported for *n*-hexadecane and *n*-octadecane miniemulsions [2, 3]. Various workers (e.g., Povey et al. [5]) have suggested that there are two populations of lipid in an emulsion droplet. The lipid closest to the surface would be mixed with the alkyl tails of the surfactant and have a lower melting point (corresponding to the minor peak in DSC) while the remaining core lipid is effectively pure and would melt at a higher temperature (corresponding to the major peak in the DSC). We suggest that the minor peak seen here corresponds to the surface lipid and has a lower melting point while the large peak corresponds to the purer lipid in the core of the droplets. In smaller droplets there is a higher proportion of the lipid at the surface, so the ratio of the size of the smaller to larger peak increases.

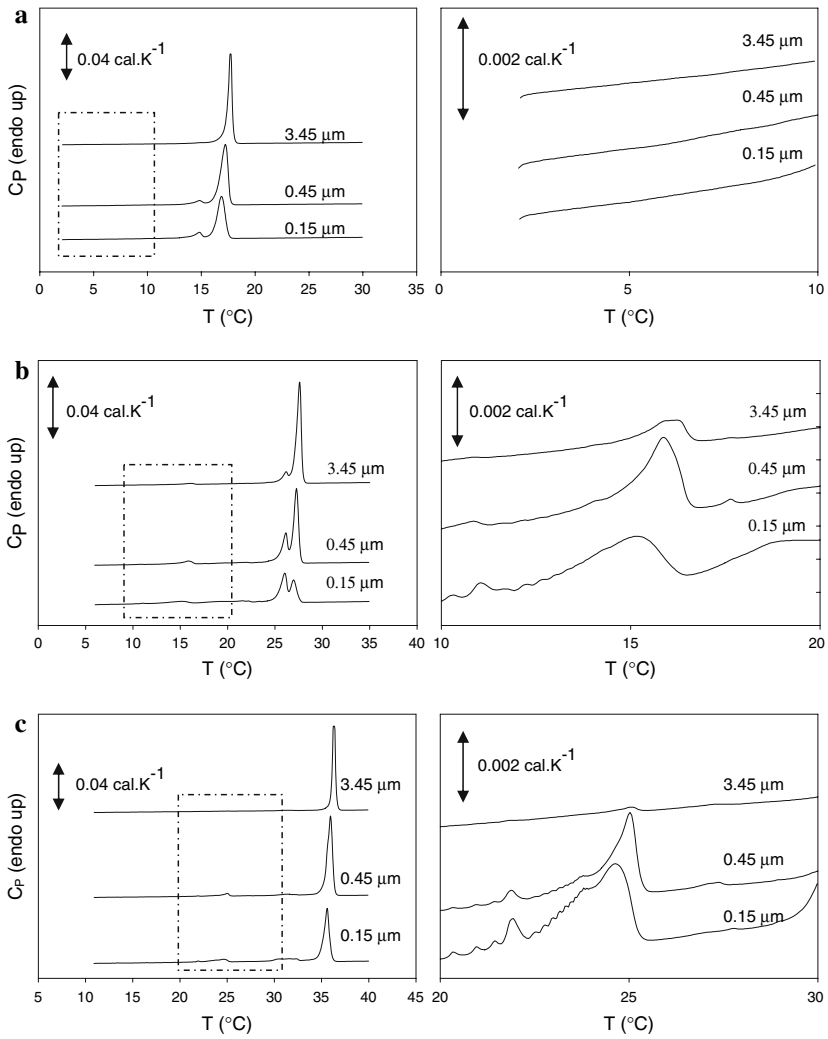

Fig. 1 Heating thermograms for 0.25% emulsions of **a** C_{16}, **b** C_{18}, **c** C_{20} stabilized by 1% Tween 20 recorded at a scanning rate of 10 °C h^{-1}. The figures to the *right* are higher resolution zooms of the *boxed area* of the main, data sets shown on the *left*

The C_{18} droplets melted at a higher temperature than the C_{16} droplets because of the stronger intermolecular forces between the larger alkanes (Fig. 1b). However, similar trends were seen in the data, i.e., a single bimodal melting peak with the proportion of the enthalpy in the lower-temperature peak decreasing with increasing droplet size). The Tween-stabilized C_{20} droplets melted at still higher temperatures, but in this case, the minor peak was less pronounced (Fig. 1c).

In the sodium caseinate stabilized emulsions (Fig. 2), the major melting peak occurred at a similar temperature to the corresponding Tween-stabilized emulsions, but there was only a single peak rather than the bimodal peak seen with Tween-stabilized emulsions. This is consistent with our hypothesis that the minor peak in the Tween-stabilized emulsions is due to the lipid mixed with surfactant alkyl groups. Proteins lack the long hydrophobic chains of surfactant and sodium caseinate is known to have little effect on the crystallization properties of lipid droplets [9, 10]. Consequently, in the caseinate stabilized emulsions there is only one population of lipid and a single DSC peak. The end point temperature for the melting of the emulsion samples was not influenced by the type of surfactant used and in each case was close to the tabulated values of the thermodynamic melting points [11].

There was a second, minor endothermic peak for the Tween stabilized C_{18} and C_{20} droplets at around 15 °C and 25 °C, respectively (Fig. 1b, c). The peak was detectable but much smaller in the corresponding caseinate-stabilized droplets and occurred at a similar temperature in each case (Fig. 2). No corresponding minor peak was seen in the C_{16} emulsions. To increase the resolution of this small peak we repeated the experiments with more concentrated emulsions (5 wt% C_{18} or C_{20}, d_{32} = 0.52 μm) (Fig. 3). (Because more of the lipid was going through the transition in this case it was possible to resolve greater detail although it was not possible to simultaneously measure the major peak due to limitations in the dynamic range of the instrument.)

Because the position of the minor peak approximately corresponded to the major melting endotherm of the next

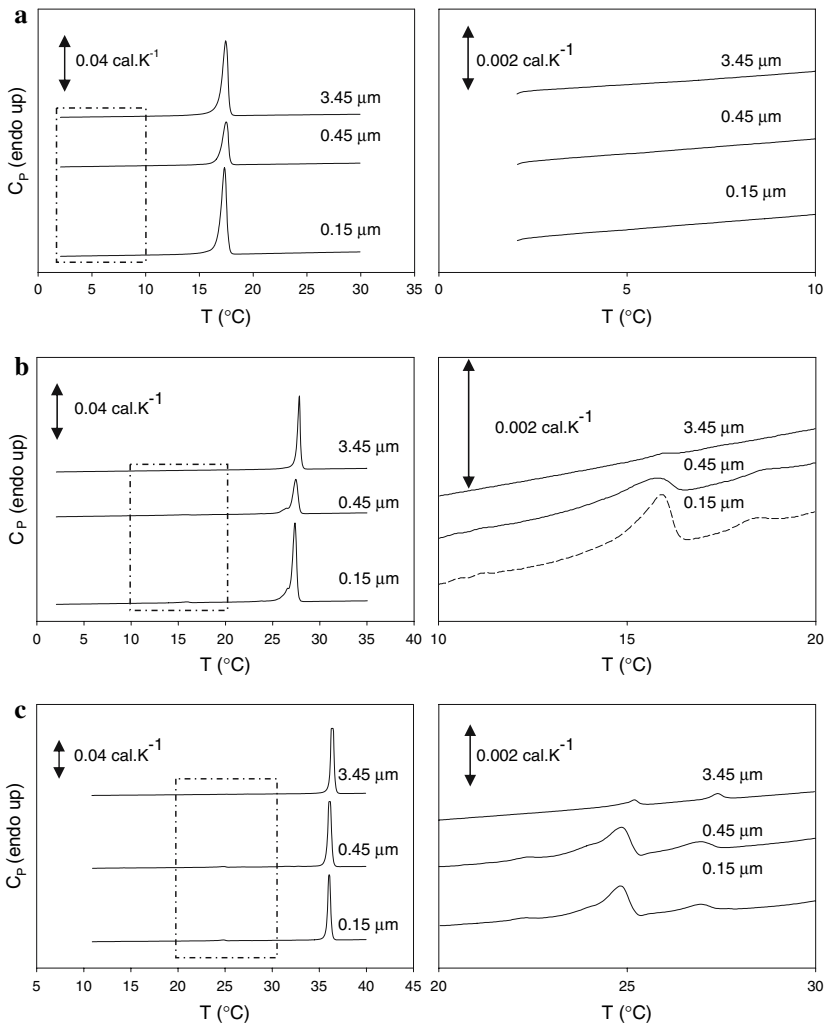

Fig. 2 Heating thermograms for 0.25% emulsions of **a** C_{16}, **b** C_{18}, **c** C_{20} stabilized by 0.5% sodium caseinate recorded at a scanning rate of 10 °Ch^{-1}. The figures to the *right* are higher resolution zooms of the *boxed area* of the main, data sets shown on the *left*

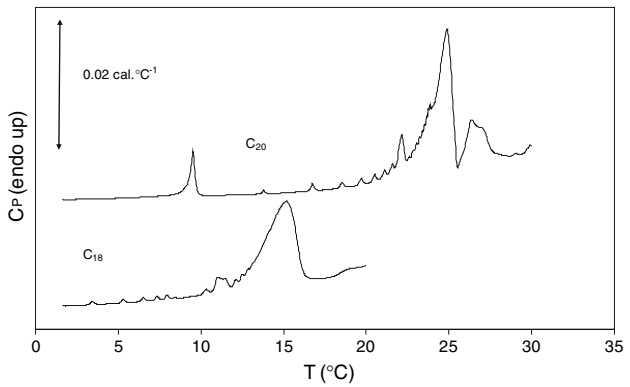

Fig. 3 Heating thermograms for 5% emulsions of C_{18}, C_{20} stabilized by 1% Tween 20 (d_{32} = 0.52 μm) recorded at a scanning rate of 10 °C h^{-1}. Data are similar to Fig. 1, but the more concentrated emulsion reveals detail of the crystal-rotator transition

smaller even *n*-alkane used, we initially suspected it could be due to the presence of a contaminant. However, mixtures of similarly-sized alkanes (i.e., C_{16} and C_{18} and C_{18} and C_{20}) co-crystallize with a melting point between the melting points of the pure components and not as independent phases (data not shown). We therefore attribute the minor peak to a solid-solid phase transition, and tentatively attribute it to the melting of a crystal phase (probably triclinic according to [3]) to form a rotator phase. A rotator phase has been previously observed in these alkanes as an intermediate between the liquid and crystalline phases [12, 13]. Montenegro and Landfester [3] used X-ray diffraction to show that transition from the stable crystalline phase to the rotator phase occurred at 15.3 °C for C_{18} emulsions (d = 125 nm), and at 24.1 °C for C_{20} emulsions (d = 129 nm). The end points of the thermal transitions reported here occurred at similar temperatures (17 and 26 °C), respectively, despite the slower scanning rate (10 °C h^{-1} against the 300 °C h^{-1} used by Montenegro and Landfester [3]). Sirota and Herhold [12, 13] used a comparable scanning rate to the one used here (i.e., 3 °C h^{-1}) in their X-ray studies of rotator phase formation in bulk alkanes, however in that work the phase transitions occurred at 27 and 32 °C, respectively. Montenegro and Landfester [3] did not observe a rotator phase for bulk or emulsified C_{16}.

Ueno and co-workers [6] saw a similar minor DSC peak a few degrees below the major crystallization/melting peak in emulsified *n*-hexadecane (φ = 20%, 0.9 μm; octadecane and eicosane were also studied but the data were not reported) stabilized by 1% Tween 20 but only in the presence of a hydrophobic additive. Alkanes typically crystallize in the triclinic form but the additive favored alternative crystal habits and, using coupled X-ray measurements, these authors were able to attribute the minor peak to a polymorphic phase transition. They saw no evidence of a rotator phase, perhaps because their scanning rate was relatively fast (2 °C min^{-1}) or due to a lack of sensitivity in their measurement apparatus. We do not believe the polymorphic phase transition detected by Ueno et al. [6] is responsible for the minor peak in our work as although we used the same lipid and surfactant we did not use the additive.

Cooling Thermograms

Cooling thermograms for C_{18} and C_{20} are shown in Figs. 4, 5 for Tween 20 and sodium caseinate stabilized samples, respectively. (Because C_{16} has a crystallization onset of approximately 2 °C, and the microcalorimeter used cannot safely be cooled below 0 °C, the main crystallization peak could not be observed fully using this apparatus and is not reported here. However, by holding all samples for 30 min at 0.5 °C we are confident that the C_{16} droplets were completely crystallized prior to beginning the heating cycle.) In most respects, the patterns seen in melting were repeated in reverse on cooling. As expected, there was an offset of about 10–15 °C between the melting and crystallization points of the emulsified lipids because the finely dispersed oil must largely nucleate homogeneously [14]. Interestingly, there was a small peak in the large caseinate stabilized C_{20} droplets close to the melting point of the fat (i.e., less supercooling). This is probably because a significant fraction of the largest droplets contained a nucleation catalyst and therefore could nucleate heterogeneously at a higher temperature [10].

The caseinate stabilized droplets crystallize about 1 °C above the corresponding Tween stabilized droplets (Figs. 4, 5). This may be related to our earlier suggestion that the hydrophobic tails of the Tween act as an impurity in the oil and depress its crystallization temperature. However, perhaps due to differences in cooling rate, this observation is different from those of Skoda and Van den Tempel [9] and Palanuwech and Coupland [10] who noted that Tween-stabilized emulsions tended to crystallize at higher temperatures than caseinate-stabilized droplets.

In some Tween-stabilized emulsions (notably C_{20} but also C_{18}) there was a small shoulder approximately 1.5 °C after the major crystallization peak. This minor peak was not identified in earlier studies perhaps due to the superior sensitivity of the instrument used here and the slow heating rates. We suggest that this small peak corresponds to the freezing of the surface monolayer where freezing temperature was depressed due to the protrusion of Tween alkyl chains. Despite this, most of the main crystallization peaks were unimodal, presumably because due to the deep supercooling, once crystallization had been initiated it rapidly spread throughout the droplet. Increasing particle sizes reduced the relative significance of this minor peak because of a reduction in surface: volume ratio of the lipid.

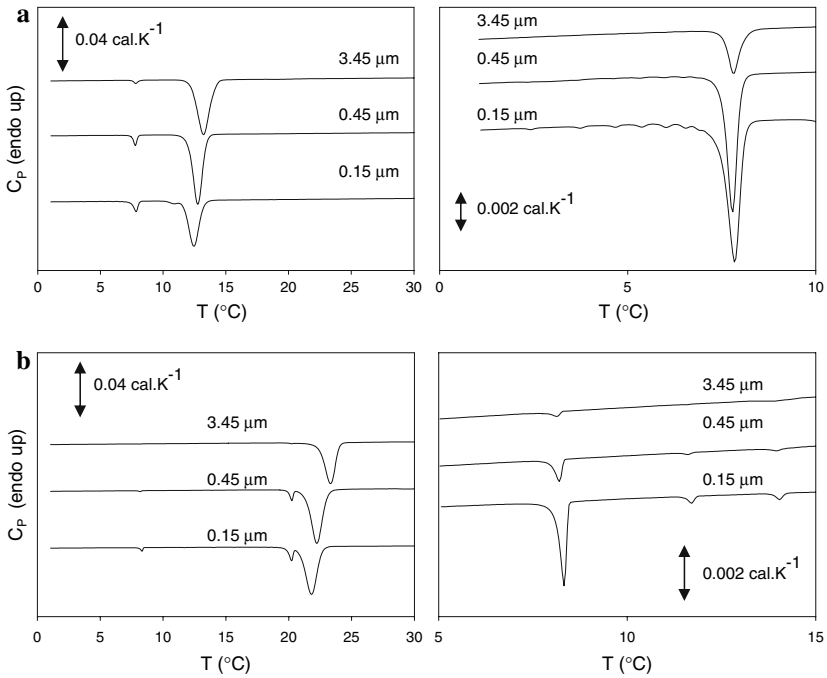

Fig. 4 Cooling thermograms for 0.25% emulsions of **a** C_{18}, **b** C_{20} stabilized by 1% Tween 20 recorded at a scanning rate of 10 °C h^{-1}. The figures to the *right* are higher resolution zooms of the *boxed area* of the main, data sets shown on the *left*

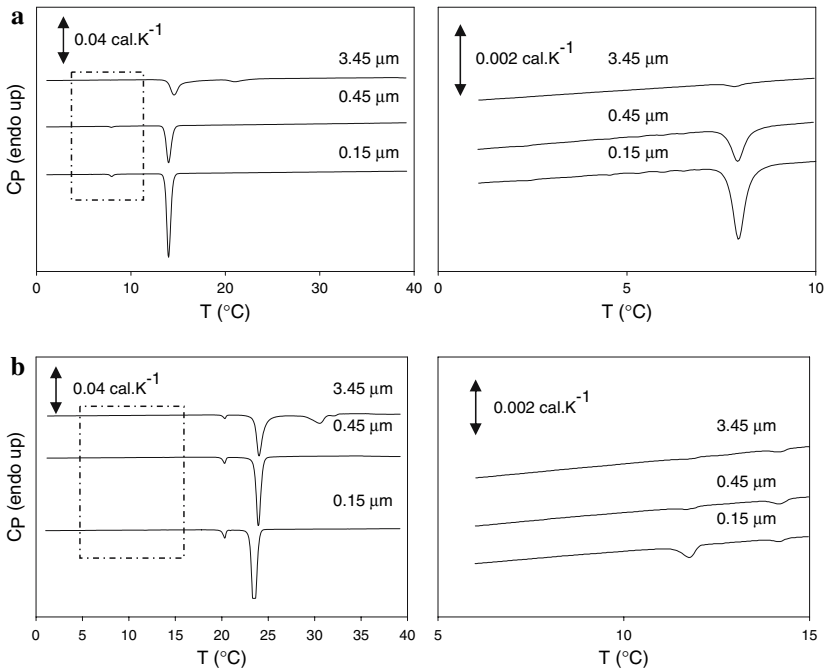

Fig. 5 Cooling thermograms for 0.25% emulsions of **a** C_{18}, **b** C_{20} stabilized by 0.5% sodium caseinate recorded at 10 °C h^{-1}. The figures to the *right* are higher resolution zooms of the *boxed area* of the main, data sets shown on the *left*

There was a smaller exothermic peak approximately 4–6 °C below the major peaks for all samples (Figs. 4, 5). The position of the peak was unaffected by the type of surfactant or the droplet size but the size of the peak decreased with increasing droplet size (and was largely absent in the largest droplets). These minor peaks were larger for the Tween-stabilized emulsions than for the caseinate-stabilized emulsions and can mostly be attributed to the interactions between the emulsifier and oil molecules. Reducing the droplet size increases the surface area and can be expected to increase the extent of these interactions. The symmetry between the properties of this peak and the properties of the minor endotherm seen on heating, leads us to attribute it to a rotator-crystal phase transition. We hypothesize that the major peak is a liquid to rotator phase transition and the minor peak is a rotator to crystal

transition. It is possible that the absence of a minor crystal-rotator phase transition on heating C_{16} droplets is not an intrinsic property of the smaller lipid but rather because we were not able to cool those samples far enough to convert them into the low temperature crystal form. In Fig. 6, we present a DSC melting scan (10–35 °C) for an octadecane sample. Small droplets (d_{32} = 0.2 μm) were selected to make any minor peaks more pronounced. Since the sample was not cooled below the rotator phase transition temperature (approximately 7.8 °C), no rotator phase transition peak was observed. Extrapolating from the larger lipids, we expect the rotator to crystal transition in the C_{16} would occur between about –5 to –10 °C.

Previously, Shinohara et al. [15] noted that hexadecane droplets (mean size 32.6 μm) crystallize into the triclinic phase through the transient rotator phase. Their results were slightly different than that of ours, since rotator to triclinic phase transitions in our DSC measurements were always characterized with a separate minor peak while in their work were seen as a small shoulder within the major DSC peak (i.e., no surface freezing). Due to instrumental limitations, we were unable to observe the rotator phase transitions in hexadecane emulsions. This difference could be in part be explained by the difference in particle size.

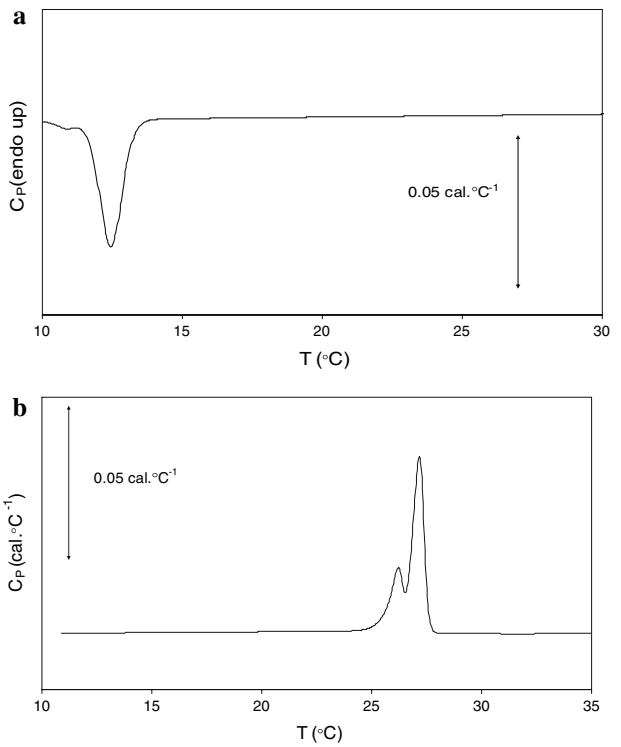

Fig. 6 Thermograms of a 0.25% C_{18} emulsion of by 1% Tween 20 (d_{32} = 0.2 μm). Samples were **a** cooled to 10 °C at 10 °C h^{-1} then **b** reheated to 35 °C at the same rate

Ultrasonic Attenuation Measurements

Ultrasonic attenuation (at 2.25 MHz) of *n*-alkane emulsions stabilized with Tween 20 and sodium caseinate were measured as a function of temperature during heating (Figs. 7, 8) and cooling (data not reported). The attenuation coefficient of the emulsions with larger droplets (i.e., 3.45 μm) was low (<10 Np m^{-1}) and could not be reliably

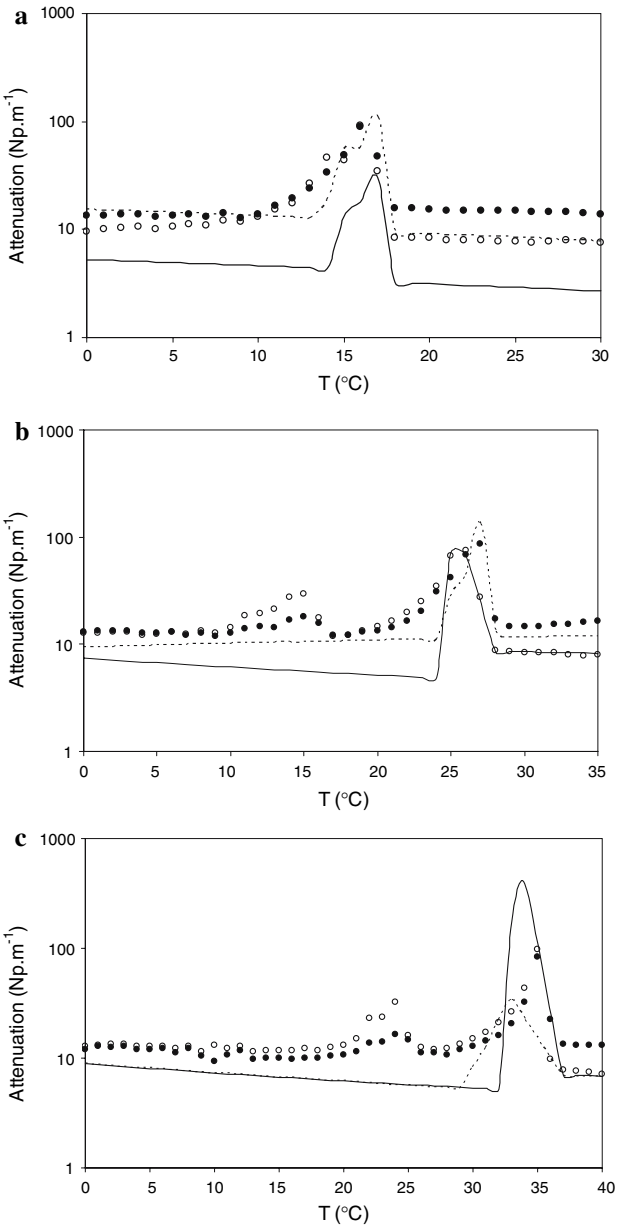

Fig. 7 Ultrasonic attenuation as a function of temperature during heating (6 °C h^{-1}) of 3% emulsions (*open circles* 0.15 μm, *filled circles* 0.45 μm) of **a** C_{16}, **b** C_{18}, **c** C_{20} stabilized by 1% Tween 20. *Lines* represent predictions from scattering theory (see text for details). *Broken lines* are used for 0.15 μm samples, *solid lines* are used for 0.45 μm samples

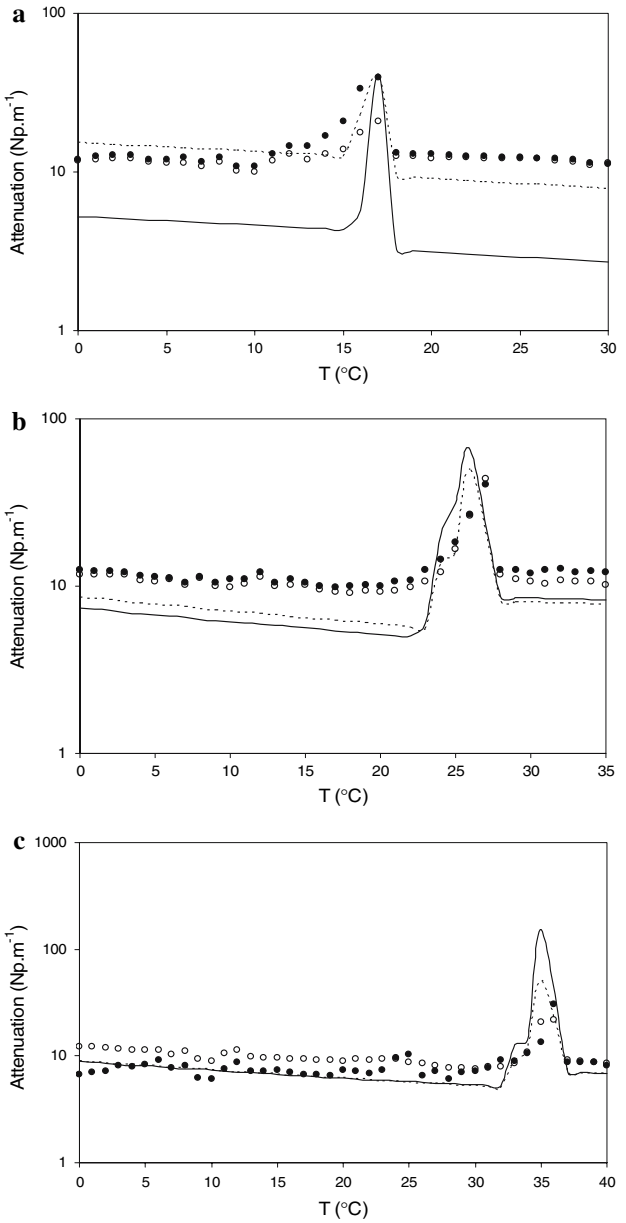

Fig. 8 Ultrasonic attenuation as a function of temperature during heating (6 °C h^{-1}) of 3% emulsions (*open circles* 0.15 μm, *filled circles* 0.45 μm) of **a** C_{16}, **b** C_{18}, **c** C_{20} stabilized by 0.5% sodium caseinate. *Lines* represent predictions from scattering theory (see text for details). *Broken lines* are used for 0.15 μm samples, *solid lines* are used for 0.45 μm samples

measured by this technique so the data are not reported. The attenuation of solid and liquid droplets was largely temperature independent and unaffected by the nature of the interfacial material. Importantly there were excess attenuation peaks during heating at temperatures corresponding to the major and minor melting peaks seen in the DSC thermograms (Figs. 1, 2). The maximum peak attenuation was always the lowest in the largest droplets and was always less in the caseinate-stabilized emulsions compared to the Tween-stabilized emulsions. There were no peaks corresponding to the crystallization of the emulsion droplets on cooling (data not shown).

The measured ultrasonic attenuation of an emulsion has contributions from the intrinsic attenuation of the component phases and from scattering by the droplets. The droplets pulsate and oscillate in the passing pressure wave, scattering sound in different directions and converting a proportion of the ultrasonic energy to heat as the droplet movement is not elastic. Good theoretical expressions have been developed for all of these terms and it is possible to predict the ultrasonic properties of an emulsion as a function of the physical properties of the component phases and the size and number of droplets [16]. Ultrasonic attenuation (unlike ultrasonic velocity) is only slightly affected by changes in temperature and even though the physical properties of solid and liquid droplets are different, ultrasonic attenuation is typically only slightly affected by droplet melting (i.e., <2 Np m^{-1}). However, during the phase transition the changing solid fat content means the instantaneous specific heat of the lipid phase is very much higher as it now includes a contribution from the enthalpy of fusion. By incorporating an effective value of specific heat (and by a similar logic density and thermal expansion coefficient) into scattering theory, we have been able to model the attenuation peaks seen during the melting of Tween stabilized *n*-octadecane emulsions [7]. Corresponding attenuation peaks are not seen during crystallization as the droplets are deeply supercooled before nucleation so crystallization is complete before a measurement can be made. We use the same theory here to model the attenuation during due to the melting of a larger set of emulsions including a variety of *n*-alkanes (C_{16}, C_{18}, and C_{20}), droplet sizes (0.15, and 0.45 μm) and emulsifying agents (Tween 20 and sodium caseinate). Our theory shows reasonable agreement with the experimental data for all of these systems (Figs. 7, 8).

The Tween-stabilized droplets had a higher excess attenuation on melting than the corresponding caseinate droplets. The excess attenuation observation is primarily due to the co-existence of solid and liquid alkane molecules in the droplets. We argued from our DSC data that there is evidence that the surface lipid in the Tween-stabilized emulsion is mixed with the alkyl tails of the surfactant and tends to remain liquid over a wider temperature range and this phenomenon could also be responsible for the greater attenuation in these samples. Furthermore, the peaks are larger for smaller droplets where the proportion of the lipid affected by the interface is greater.

A similar attenuation peak was observed at the temperatures where the crystalline phase converted to a rotator phase as the melting enthalpy needed for the crystal-rotator

transition and the density differential between the phases contributes to the increased attenuation of the samples. The attenuation peak is again larger for the Tween-stabilized samples than for the caseinate-stabilized samples and increased with decreasing particle size.

Conclusions

In the present work, we used microcalorimetry and ultrasonic attenuation measurements to investigate the thermal transitions in emulsified alkanes during cooling and heating as a function of alkane chain length, surfactant type and droplet size. The significant conclusions of this work are that (1) alkane droplet crystallization and melting is a two-step process proceeding via an intermediate, probably rotator, phase, (2) there is an excess ultrasonic attenuation during droplet melting that decreases with increasing droplet size, and this finding is coherent with our extended scattering theory approach, (3) surfactant molecules can act as crystal modifiers or stabilizers during the crystallization and melting of emulsified lipids, and affect the magnitude of the thermal transitions and excess ultrasonic attenuation.

Although our measurements are of emulsions of simple alkanes, the physical transformations in the lipid responsible for the excess attenuation will also occur in more complex, lipid-continuous systems such are margarine and chocolate. Semi-crystalline lipids such as these frequently have unexpectedly high ultrasonic attenuation [17] and while this can be attributed by scattering from the structural elements, it seems reasonable that the excess attenuation described here could also contribute. If this is the case, we would expect fats with a broad melting curve (e.g., milkfat in butter) would have a lower excess attenuation than those with a steeper melting curve (e.g., cocoa butter in chocolate) at a similar solids level. Solid fat content can be calculated from ultrasonic velocity measurements using a volume-weighted average of the properties of the solid and liquid phases but ultrasonic attenuation, while easily measured simultaneously, is not often used in these sensors [18]. If the excess attenuation theory described here can be validated for complex, lipid continuous samples it may be possible to combine velocity and attenuation measurements to give a more complete ultrasonic characterization of semicrystalline lipids. Furthermore, as originally suggested by McClements et al. [17], the dynamics of melting can be determined from the frequency dependence of attenuation data.

Acknowledgments The project was supported by the National Research Initiative of the USDA Cooperative State Research, Education and Extension Service, grant number 2003-35503-13852.

References

1. Coupland JN (2004) Crystallization in emulsions. Curr Opin Colloid Interface Sci 7(5–6):445–450
2. Montenegro R, Antionetti M, Mastai Y, Landfester K (2003a) Crystallization in miniemulsion droplets. J Phys Chem B 107(21):5088–94
3. Montenegro R, Landfester K (2003b) Metastable and stable morphologies during crystallization of alkanes in miniemulsion droplets. Langmuir 19(15):5996–6003
4. Katsuragi T, Kaneko N, Sato K (2001) Effects of addition of hydrophobic sucrose fatty acid oligoesters on crystallization rates of *n*-hexadecane in oil-in-water emulsions. Colloids Surf B 20(3):229–237
5. Povey MJW, Hindle SA, Aarflot A, Hoiland H (2006) Melting point depression of the surface layer in *n*-alkane emulsions and its implications for fat destabilization in ice cream. Cryst Growth Des 6(1):297–301
6. Ueno S, Hamada Y, Sato K (2003) Controlling polymorphic crystallization of n-alkane crystals in emulsion droplets through interfacial heterogeneous nucleation. Cryst Growth Des 3(6):935–939
7. Gülseren İ, Coupland JN (2007) Excess ultrasonic attenuation due to solid-solid and solid-liquid transitions in emulsified octadecane. Cryst Growth Des 7(5):912–918
8. Kraack H, Sirota EB, Deutsch MJ (2000) Measurements of homogeneous nucleation in normal-alkanes. J Chem Phys 112(15):6873–85
9. Skoda W, van den Tempel M (1963) Crystallization of emulsified triglycerides. J Colloid Sci 18(6):568–584
10. Palanuwech J, Coupland JN (2003) Effect of surfactant type on the stability of oil-in-water emulsions to dispersed phase crystallization. Colloids Surf A 223(1):251–262
11. Gallant RW, Yaws CL (1993) Physical properties of hydrocarbons and other chemicals, vol 3. Gulf Publishing, Houston
12. Sirota EB, Herhold AB (2000) Transient rotator phase induced nucleation in *n*-alkane melts. Polymer 41(25):8781–89
13. Sirota EB, Herhold AB (1999) Transient phase-induced nucleation. Science 283(5401):529–532
14. Dickinson E, McClements DJ (1995) Advances in food colloids. Blackie Academic and Professional, New York
15. Shinohara Y, Kawasaki N, Ueno S, Kobayashi I, Nakajima M, Amemiya Y (2005) Observation of the transient rotator phase of *n*-hexadecane in emulsified droplets with time-resolved two-dimensional small- and wide-angle X-ray scattering. Phys Rev Lett 94:(097801-1)–(097801-4)
16. McClements DJ, Coupland JN (1996) Theory of droplet size distribution measurements in emulsions using ultrasonic spectroscopy. Colloids Surf A 117(1):161–170
17. McClements DJ, Povey MJW, Dickinson E, (1993) Absorption and velocity dispersion due to crystallization and melting of emulsion droplets. Ultrasonics 31(6):433–437
18. McClements DJ, Povey MJW (1987) Solid fat content determination using ultrasonic velocity measurements. Int J Food Sci Technol 22(5):491–499